Evidence for Psammotermes allocerus termite nests as refugium for plant pathogenic microbes: a contribution to generation and maintenance of fairy circles in the Namib Desert

Authors: Yurkov, A., Pascual, J., Sikorski, J., Geppert, A., Gunter, F., Huber, K.J., Jürgens, N., Overmann, J.

Published by: Biodiversity & Ecology, 7, 254 – 273

Klaus Hess Publishers, Göttingen & Windhoek

DOI: 10.7809/b-e.00370

8.4 Evidence for *Psammotermes allocerus* termite nests as refugium for plant pathogenic microbes: a contribution to generation and maintenance of fairy circles in the Namib Desert

Authors: Andrey Yurkov[a#], Javier Pascual[a#], Johannes Sikorski[a], Alicia Geppert[a], Felicitas Gunter[b], Katharina J. Huber[a], Norbert Jürgens[b], Jörg Overmann[a*]

[#] Shared first authorship, these authors contributed equally

[a] Leibniz Institute DSMZ-German Collection of Microorganisms and Cell Cultures. Braunschweig. Germany.
[b] Institute of Plant Science and Microbiology. University of Hamburg. Hamburg. Germany.

* Correspondence: J. Overmann. Leibniz-Institut DSMZ-Deutsche Sammlung von Mikroorganismen und Zellkulturen GmbH. Inhoffenstraße 7B. 38124 Braunschweig. Germany. Tel: +49-531-2616-352. Fax: +49-531-2616-418. Email: joerg.overmann@dsmz.de

Recommended citation:
Yurkov, A., Pascual, J., Sikorski, J., Geppert, A., Gunter, F., Huber, K.J., Jürgens, N., Overmann, J. (2022) Evidence for *Psammotermes allocerus* termite nests as refugium for plant pathogenic microbes: a contribution to generation and maintenance of fairy circles in the Namib Desert. In: Schmiedel, U. & Finckh, M. (Eds.) Fairy circles of the Namib Desert – Ecosystem engineering by subterranean social insects. *Biodiversity & Ecology.* 7. 254–273. DOI: 10.7809/b-e.00370

Abstract

Fairy circles are circular, barren structures in dry grasslands and the mechanisms generating and maintaining them are currently under intense discussion. Here, we analysed bacterial and fungal communities in Namib Desert fairy circle soils, in the tapetum lining of termite nests, the gut of the prevailing sand termite *Psammotermes allocerus,* and also in the neighbouring grass plants. The total and active microbial communities were analysed through amplicon sequencing of both DNA and RNA extracts, respectively, species-specific PCRs, and through cultivation of bacteria and fungi from the various samples. In the sandy soils, the active bacterial communities were substantially different from the total communities, which suggested the fairy circle soils to be highly selective environments in comparison to other drylands or even temperate soils. This appears to be even more true for fungi as amplification of fungal genes from RNA extracts was not possible. However, we observed a large diversity among cultured fungal species in comparison to cultured bacterial species, specifically in tapetum samples. Our results support the hypothesis that *Psammotermes allocerus* acts as a vector for plant pathogenic fungi and that their nests below the bare patches of fairy circles provide a refugium for the fungal plant pathogens.

Introduction

Drylands are found in tropical and temperate latitudes, account for about 40% of the terrestrial surface of the Earth, and accumulate approximately 25% of the global soil carbon (Safriel et al. 2005). The hyper-arid Namib Desert may represent the oldest desert of the world and comprises the world´s driest regions with extreme temperature conditions. Therefore, the Namib Desert is of particular interest for elucidating biological adaptations to desert ecosystems (Armstrong et al. 2016; Cowan et al. 2020). With the advent of high throughput nucleotide sequencing technology, the composition and role of soil microbial communities in drylands has attracted increased interest (Delgado-Baquerizo et al. 2017; Maestre et al. 2015; Steven et al. 2021). Most of the previous studies relied on molecular analyses of DNA extracts and thus targeted total microbial communities but at the same time also the large fraction of relic DNA (Carini et al. 2016), or inactive and dormant cells (Kuzyakov & Blagodatskaya 2015). Only few studies of the microbial diversity in dryland soil have so far focused on active bacterial communities through analysis of extracted RNA (Huber et al. 2022; León-Sobrino et al. 2019 and, more importantly, attempted to isolate and characterize microbial taxa therein (Huber et al. 2017; Huber & Overmann 2018; Huber et al. 2022; Pascual et al. 2015a, 2015b).

Fairy circles are circular, barren structures in dry grasslands (see also the other contributions to this book). The fairy circle landscape primarily consists of a considerable number of very old, well-established fairy circles which reach diameters of up to 40 m and of new fairy circles that only appear after years with abundant rainfall (compare Chapter 4). There is a continuing debate over the mechanism of formation of fairy circles (Meyer et al. 2021; Sahagian 2017), specifically with respect to the well-studied ones in the Namib Desert. Two major hypotheses prevail, which either propose a self-organization through interactions involving plants, soil, wind, and water (Getzin et al. 2016; Ravi et al. 2017) or suggest a critical role of social termites (specifically, *Psammotermes allocerus*) which engineer patches from a centre through both, building subterranean nests and herbivory, resulting in an substantially increased water storage in bare patches (Jürgens 2013; Jürgens et al. 2015). The role of microorganisms in the formation and maintenance of fairy circles is largely unknown despite their key role for eco-

system processes and nutrient cycling in other soils. Initial studies have demonstrated an effect of different habitat zones of fairy circles on bacterial, fungal and archaeal communities (Van der Walt et al. 2016).

In the present study, the analysis of microbial communities was extended beyond the different habitat zones (inside the fairy circles bare patch, perennial belt and matrix) to include, for the first time, also the different constituents of the tapetum material lining the termite nests, and also the gut content of the termite *Psammotermes allocerus*. Moreover, we specifically assessed active bacterial and fungal communities through analysis of RNA extracts and through the cultivation of bacteria and fungi from the tapetum material. The microbial taxa which were thus identified as potentially active most likely contribute to the formation and the maintenance of the fairy circles, which provides novel insights into the ecology of these peculiar landscape structures.

Material and Methods

Study site and sample collection

Soils samples from five fairy circles (FC1, FC4, FC5, FC8 and FCDHg) were collected from the Southern Namib at the farm Dieprivier, in April 2013 (Fig. 8.4.1A, Table 8.4.1). FC1, FC4 and FC5 were located within a distance of up to 25.9 km, whereby FC8 and FCDHg represented the most distant ones (min. distance to closest FCs, 1982 m and 468 m, respectively). The five fairy circles showed different diameters at the time of the sampling (min = 2.8 m; max = 3.7 m). Each fairy circle was sampled along a spatial transect which included two samples collected in the centre of the circle (CT), and another one at half the distance of the radius of the fairy circle (HD), and also two samples outside the bare patch, one from the perennial belt (PB) of *Stipagrostis ciliata* directly adjacent to the bare patch, and another sample from the surrounding vegetation matrix (MT) (Fig. 8.4.1B). Soil samples for molecular analyses were aseptically collected directly into Falcon tubes containing LifeGuard Soil Preservation Solution (Qiagen, Hilden Germany). Afterwards, the Falcon tubes were kept continuously at -20°C until nucleic acid extraction in the laboratory. Soil samples for cultivation studies were collected and kept in plastic bags transported back to the laboratory and maintained at 4°C until analysis.

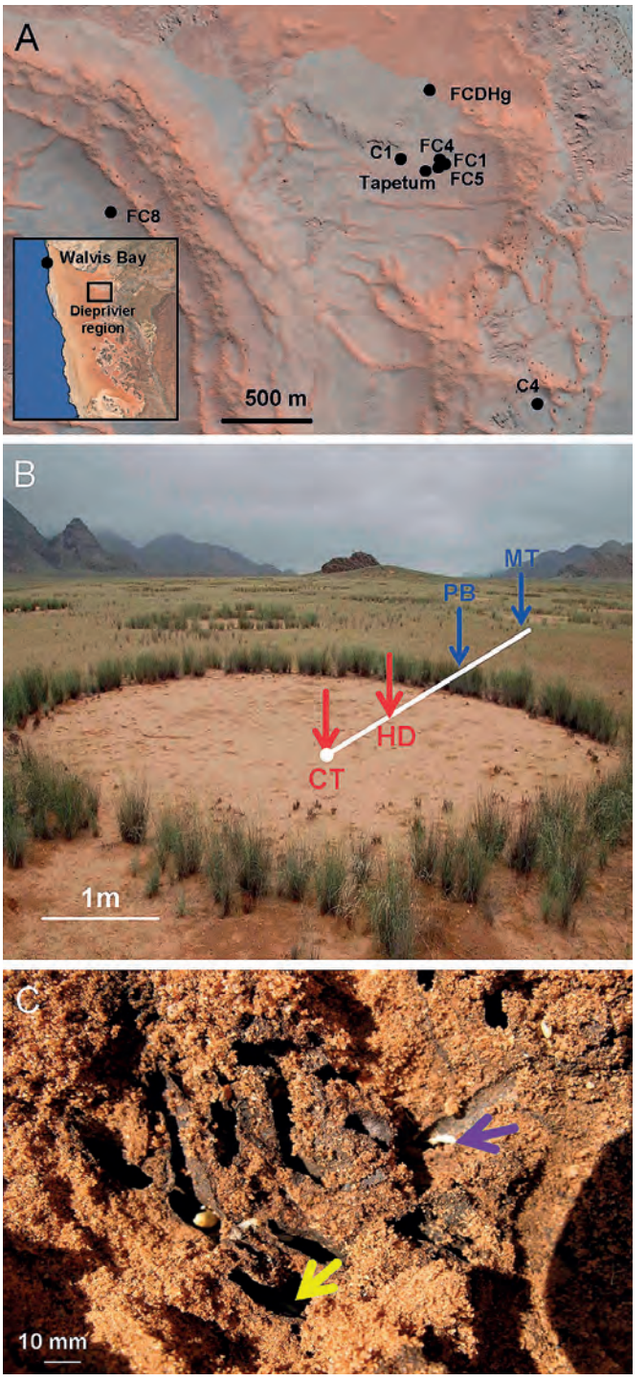

Figure 8.4.1 A, B and C: Location and structure of sampling sites.
A: Geographical location of the fairy circles analysed in this study in Dieprivier region of Namib. Soils were sampled from 5 fairy circles (FC1, FC4, FC5, FC8 and FCDHg), tapetum samples from a single FC (FC-Tapetum) and termites from 14 fairy circles placed in two distant regions (Termites-C1 and Termites-C4).
B: Spatial transect of the soil sampling locations along an individual fairy circle. The transect comprised two sampling points inside each FC, the centre of the circle (CT), and the half distance of the radius (HD), and also two sampling points outside in the perennial belt (PB) and matrix (MT). The surrounding perennial belt and matrix was covered by *Stipagrostis ciliata* and *Stipagrostis obtusa*, respectively.
C: Dark organic material lining the termite tunnel system (so-called tapetum; yellow arrow). A sand termite *Psammotermes allocerus* is shown by a dark violet arrow.

Table 8.4.1: Geographical origin of fairy circle samples

Fairy Circle	Sample	Transect Position	Data of collection	Latitude	Longitude	Altitude (m)
FC1	Soil	Inside FC (CT)	04-2013	-24.1310500	15.895870	1050
FC1	Soil	Inside FC (HF)	04-2013	-24.1310500	15.895870	1050
FC1	Soil	Outside FC (PB)	04-2013	-24.1310500	15.895870	1050
FC1	Soil	Outside FC (MT)	04-2013	-24.1310500	15.895870	1050
FC4	Soil	Inside FC (CT)	04-2013	-24.1310900	15.895670	1050
FC4	Soil	Inside FC (HF)	04-2013	-24.1310900	15.895670	1050
FC4	Soil	Outside FC (PB)	04-2013	-24.1310900	15.895670	1050
FC4	Soil	Outside FC (MT)	04-2013	-24.1310900	15.895670	1050
FC5	Soil	Inside FC (CT)	04-2013	-24.1311200	15.895640	1050
FC5	Soil	Inside FC (HF)	04-2013	-24.1311200	15.895640	1050
FC5	Soil	Outside FC (PB)	04-2013	-24.1311200	15.895640	1050
FC5	Soil	Outside FC (MT)	04-2013	-24.1311200	15.895640	1050
FC8	Soil	Inside FC (CT)	04-2013	-24.132380	15.876730	1021
FC8	Soil	Inside FC (HF)	04-2013	-24.132380	15.876730	1021
FC8	Soil	Outside FC (PB)	04-2013	-24.132380	15.876730	1021
FC8	Soil	Outside FC (MT)	04-2013	-24.132380	15.876730	1021
FCDHg	Soil	Inside FC (CT)	04-2013	-24.127060	15.895940	1062
FCDHg	Soil	Inside FC (HF)	04-2013	-24.127060	15.895940	1062
FCDHg	Soil	Outside FC (PB)	04-2013	-24.127060	15.895940	1062
FCDHg	Soil	Outside FC (MT)	04-2013	-24.127060	15.895940	1062
FC-Tapetum	Tapetum	Inside FC	10-2013	-24.1312800	15.8955200	1044
C1FC2	Termite gut	Inside FC1	02-2013	-24.1312870	15.8936510	1052
C1FC3	Termite gut	Inside FC1	02-2013	-24.1311870	15.8936340	1053
C1FC4	Termite gut	Inside FC1	02-2013	-24.1311420	15.8935600	1053
C1FC5	Termite gut	Inside FC1	02-2013	-24.1312580	15.8934730	1053
C1FC6	Termite gut	Inside FC1	02-2013	-24.1313570	15.8934990	1053
C1FC7	Termite gut	Inside FC1	02-2013	-24.1313640	15.8936120	1052
C1FC8	Termite gut	Inside FC1	NA	NA	NA	NA
C4FC1	Termite gut	Inside FC4	03-2013	-24.1462520	15.9007100	1019
C4FC2	Termite gut	Inside FC4	03-2013	-24.1463200	15.9006450	1019
C4FC3	Termite gut	Inside FC4	03-2013	-24.1462070	15.9006180	1020
C4FC4	Termite gut	Inside FC4	03-2013	-24.1461710	15.9009330	1018
C4FC5	Termite gut	Inside FC4	03-2013	-24.1460460	15.9007610	1020
C4FC6	Termite gut	Inside FC4	03-2013	-24.1460880	15.9003870	1022
C4FC7	Termite gut	Inside FC4	03-2013	-24.1461920	15.9004390	1021

In addition to the soil samples, a total of eight samples of termites' nests were collected from the fairy circles of Plot 32678 at Dieprivier in October 2013. The black organic material lining the termite burrows (the so-called tapetum) was collected from nests samples and labelled as FC-Tapetum (Fig. 8.4.1C, Table 8.4.1). Nests were dissected under the stereo microscope. In the tunnel systems of termites, several dead-end compartments were discovered that contained small 2–5 mm pieces of grasses (Fig. 4.18 and Fig. 4.19, this book). During dissection, samples of grass residues and thick hyphae of fungi in the tapetum were removed and analysed separately.

Grass samples showing macroscopically visible infection symptoms in the form of purple leaf lesions were collected in the perennial belt area and transported back to the laboratory in Germany for analysis. These samples were dissected under the stereo microscope and plant inner tissues underlying the lesions were used for subsequent analyses.

Seventy-three sand termites (*Psammotermes allocerus*) were collected in February 2013 from the bare patches of 14 different fairy circles located in two separated areas of the Dieprivier region named C1 and C4 (Fig. 8.4.1A, Table 8.4.1). One to eight termites per fairy circle were sampled, including worker and soldier castes (Fig. 8.4.1C). Additionally, seventeen sand termites were collected from the matrix of the fourteen fairy circles and pooled as a single sample. All sand termites were preserved with 70% ethanol at room temperature until they were processed in the laboratory.

Microbial community analysis by cloning, high throughput sequencing and specific PCRs

Bacterial communities along fairy circle compartments, tapetum without adhering plant material, and termite guts were investigated by Illumina HiSeq amplicon sequencing of the V3 region of 16S rRNA genes. In addition, the active fraction of the edaphic bacterial community was also investigated by sequencing the cDNA generated by reverse transcription of isolated RNA. Fungal communities along spatial soil transects and tapetum samples were analysed by ITS2 Illumina HiSeq amplicon sequencing. Full details about the nucleic acid extraction, PCR amplifications, amplicon purification and high throughput sequencing have been reported previously (Carl et al. 2022; Huber et al. 2022; Sikorski et al. 2022; Tedersoo et al. 2015).

For the culture-independent analysis of fungi in grass samples from the bare patches, clone libraries were established using universal fungal PCR primers. To extract total DNA from grass, a sample was pre-treated using Matrix B and the FastPrep24 instrument (MP Biomedicals) for 60 seconds at 6.5 $m \cdot s^{-1}$. Then, the DNeasy Plant Mini Kit (Qiagen) was used following instructions of the manufacturer. The ITS region was amplified with primers ITS1F and ITS4. Amplification products were cloned into the vector pCR4-TOPO with the TOPO TA cloning kit (Invitrogen) following instructions of the manufacturer. Positive colonies were picked randomly and screened directly for inserts by performing colony PCR with vector-specific primers. A total of 100 positive clones were purified and sequenced with PCR primers. Identification of fungi from the clone library was performed as for the cultivated strains (see below).

The presence of *Curvularia* fungi in the termite guts was determined by PCR using specific primers targeting the ITS region. For this, a *Curvularia*-specific primer pair was designed with the tool Primer-BLAST (Ye et al. 2012). The newly designed pair of primers CurvuF (5′-TGTCTTTTGCGCACTTGTTGT-3′) and CurvuR (5′-TACGTATCGCATTTCGCTGC-3′) was validated *in silico* against the non-redundant NCBI GenBank database and the UNITE fungal ITS reference-trained dataset (UNITE 7.1). The specificity of the pair-primer was also tested *in vitro* by PCR using DNAs from four *Curvularia* isolates from tapetum as positive controls and other cultured *Pleosporales* as negative controls. The PCR cocktail and thermal reaction was the same as used for the ITS2 metagenomic study, except that the annealing temperature was 60°C. All reactions were done in triplicates.

Bioinformatic processing of amplicon sequence reads of microbial communities

For 16S rRNA gene sequences, raw sequences were trimmed, dimer filtered, and forward and reverse reads joined, following the protocol described elsewhere (Gossner et al. 2016; Pascual et al. 2017). Potential chimeric sequences were detected using Uchime (Edgar et al. 2011) and

removed from the datasets. Sequences were clustered into operational taxonomic units (OTUs) at 3% dissimilarity with QIIME V1.9.1 (Caporaso et al. 2010) following an open reference OTU picking strategy using UCLUST (Edgar 2010). Taxonomy was assigned using the SILVA database (v.128) (Quast et al. 2013) and employing UCLUST (Edgar 2010). Representative sequences of each OTU were aligned with the SILVA database using PyNAST (Caporaso et al. 2010) and a phylogenetic tree was constructed using FastTree2 (Price et al. 2010). This tree was used to measure the phylogenetic similarity between samples using weighted UniFrac distances (Lozupone et al. 2011). OTUs that constituted < 0.005% of reads in the total dataset were removed as recommended for Illumina generated data (Bokulich et al. 2013).

For ITS2 sequences, paired-end reads assembly, quality filtering, chimera checks, ITS2 region extraction, clustering of OTUs (3% dissimilarity), and taxonomic assignment were performed using the Pipits pipeline (Gweon et al. 2015). The taxonomic assignments of representative OTUs were based on the UNITE fungal ITS reference trained dataset, version UNITE 7.1. The 40 most frequently detected representative OTU sequences were identified employing the NCBI GenBank (https://blast.ncbi.nlm.nih.gov/) sequence database (uncultured/environmental sample sequences excluded; restricted to sequences from type material) through the megablast and blastn algorithms (Johnson et al. 2008), and in parallel employing the MycoBank (https://www.mycobank.org) sequence database. All the reads identified as belonging to Protista and plants were removed from the OTU table.

Statistical analyses

Statistical analyses of microbial communities were performed on the following groups of samples representing four different habitat types (or compartments) in fairy circles, namely (1) soil inside the bare patch (CT, HD), (2) soil outside the bare patch (PB, MT), (3) tapetum and (4) termite gut.

Alpha-rarefaction curves [iNEXT::iNEXT(q=0, datatype="abundance")] and the determination of sample coverage values [iNEXT::DatInfo()] (Chao & Jost 2012) were done with the R package iNEXT (version 2.0.12) (Hsieh et al. 2016). Based on OTUs defined at 3% sequence dissimilarity, the richness of both bacterial and fungal taxa was determined and the beta-diversity of bacterial communities analysed by Principal Coordinate Analysis (PCoA; based on weighted UniFrac and Bray-Curtis distances for bacteria and fungi, respectively) using the R packages phyloseq (version 1.16.2) and RAM (version 1.2.1.3). The alpha-gambin value characterizing species-abundance distributions (SADs) was calculated using the gambin R package (Matthews et al. 2014). Figures were constructed with the R packages ggplot2 (version 2.2.1) and ggVennDiagram (version 1.2.0).

For beta-diversity analyses of both bacterial and fungal communities, samples were normalized with the metagenomeSeq CSS (cumulative sum scaling) algorithm (Paulson et al. 2013) and further Log2 transformed (1+x) to eliminate the potential biases due to uneven sequencing depth (Costea et al. 2014). In order to analyse statistical differences between groups at beta-diversity level, PERMANOVA analyses were performed using the function adonis2() in the R vegan package and were repeated 100 times in order to account for stochastic variability during the permutation procedure (N = 999 by default) and to determine the mean *p*-value. To compare groupwise mean values of richness or SADs, the multcomp R package (version 1.4-6) [multcomp::glht(stats::aov(values ~ groups, data), mcp(groups = "Tukey"), vcov = vcovHC)] (Herberich et al. 2010) or the *t*-test [stats::t.test (); default conditions] was used

Isolation of bacterial and fungal strains from tapetum samples

For bacterial isolation, two complementary strategies were applied in order to maximize the diversity of isolated strains obtained. The first strategy applied a high-throughput cultivation approach based in liquid oligotrophic media (SSE:HD 1:10, SE/HD 1:10 and R2A 1:10), low-concentration inocula (10 or 25 bacterial cells per well, in order to outcompete less abundant but fast-growing bacteria) and extended incubation times (12 weeks), which allows to isolate difficult-to-grow bacteria (Overmann et al. 2017; Pascual et al. 2015a). The second cultivation strategy was employed to enrich biofilm-forming bacteria (i.e., bacteria which are capable of adhesion) on different solid surfaces following the methodology described by (Gich et al. 2012). The taxonomic identification was based on the full-length 16S rRNA gene (Gich et

al. 2012) using the online database EzBioCloud (Yoon et al. 2017).

Fungi were isolated from soil (bare patch), tapetum (both dark linings of the tunnels and plant residues) and grass samples. Duplicates of soil and tapetum samples were placed in 15 ml plastic tubes, suspended in sterile water (w/v) (1:5, 1:10 and 1:20) and shaken on the FastPrep24 instrument (MP Biomedicals) for 60 seconds at 6.5 $m \cdot s^{-1}$. An aliquot of 0.15 ml was plated on the surface of solid media, yeast extract–malt extract (YM) and 1:10 dilute YM media, supplemented with 200 $mg \cdot l^{-1}$ chloramphenicol to prevent bacterial growth. Grass samples were aseptically removed from the tapetum under a dissection microscope and placed on the surface of YM, potato-dextrose (PDA, Difco) and 20% (v/v) V8 (Campbell Soup Corp.) juice (DSMZ medium 310; https://mediadive.dsmz.de) agars. Foliar parasites on *Stipagrostis* collected from the perennial belt of fairy circles were cultivated by placing pieces of infected grass on PDA and V8 agars. Plates were examined after 7, 14 and 21 days of incubation. Colonies were differentiated into macro-morphological types using a stereo microscope, counted and 1-2 representatives of each colony type per plate were transferred into pure culture. Fungi (both, filamentous and yeasts) were identified using nucleotide sequences of the ribosomal ITS region and D1/D2 domains of the 26S rRNA gene (LSU) using the methodology described elsewhere (Yurkov et al. 2012). In short, the fragment was amplified with primers ITS1F and LR5 and sequenced with internal primers ITS4 and NL4. Frequently observed species of the genera *Aspergillus*, *Curvularia* and *Fusarium* were identified using nucleotide sequences of protein-coding genes *CAM*, *GAPDH* and *TEF1*. For species identification the obtained nucleotide sequences were compared with sequences deposited in the NCBI GenBank and MycoBank databases.

The probability of isolation was calculated for cultivated fungi as the number of obtained isolates from different physical replicates or plates relative to the total number of non-empty replicates.

Results and Discussion

After the filtering of the raw reads, a total of 48,804,368 and 5,049,928 high-quality 16S rRNA and ITS2 sequences were obtained, respectively. A visual inspection of the alpha-rarefaction curves (not shown) suggested a high level of sequences depth saturation. In addition, the summary statistics of the sample coverage values (Chao & Jost 2012) (min. = 0.9986, median = 0.9998, max. = 1) across all samples were remarkably high and further indicated a nearly complete coverage sequence diversity per sample.

Bacterial and fungal community composition structures

Clear differences were observed between soil samples and tapetum samples for total bacterial as well as fungal community composition based on the analysis of DNA extracts (Fig. 8.4.2 A, B). In addition, the bacterial communities from termite guts differed clearly from both the soil and tapetum samples. The different composition of bacterial communities from soil samples inside (CT and HD, Fig. 8.4.1 B) and outside of the fairy circles (PB and MT, Fig. 8.4.1 B) was substantiated by a separate ordination analysis of just these samples (Fig. 8.4.2 A, insert), demonstrating a prevailing effect of the different fairy circle compartments on total bacterial community composition. By contrast, fungal communities did not differ between habitats inside or outside of fairy circles (Fig. 8.4.2 B, insert), indicating that the different ecological conditions did not affect overall fungal community structure.

The analysis of the 16S rRNA gene transcript sequences provides insights into the composition of active bacterial communities, and it was recently shown that soil humidity and water retention capacity significantly impacts active bacteria in dryland soils (Huber et al. 2022). We, therefore, analysed active bacterial communities and compared their composition to those of the entire communities across the different habitats of the fairy circles. RNA could successfully be extracted from only eight soil samples (three out of nine inside samples, and five out of ten outside samples) whereas the RNA yield from the other samples was below detection limit. The amount of extracted RNA (on average 771 ng RNA per gram of soil) from the eight soil samples reached half of the amount of extracted DNA (on average 1473 ng DNA per gram of soil). By comparison, RNA was successfully extracted with the same extraction methodology from all of over 100 soil samples in an accompanying study on Subsaharan Kalahari soils (Huber et al. 2022) and

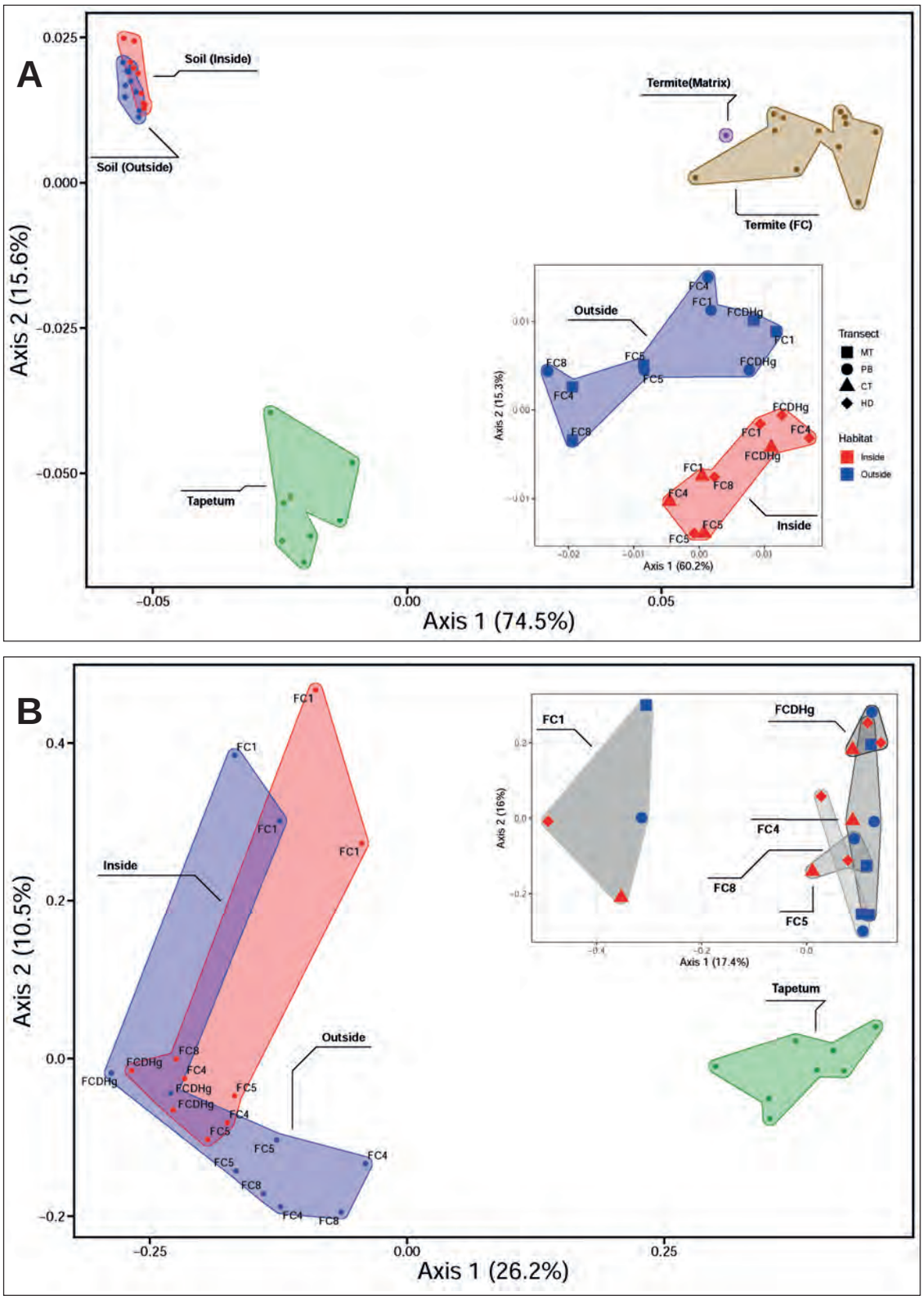

Figure 8.4.2 A, B: PCoA ordination plots of bacterial (A) and fungal (B) community structures. Each dot represents a sample using the community structure at OTU resolution (3% dissimilarity level). (A) Bacterial community structure (PCoA, weighted unifrac distances). (B) Fungal community structure (PCoA, Bray-Curtis distances at the resolution of OTUs). For both (A) and (B), the samples are represented in the main figure by filled circles. For both (A) and (B) the inserts show a re-calculated PCoA analysing only the soil samples. The shapes of the points in the inserts reflect position of the sample in the transect, see legend to insert of Figure 8.4.2 A.

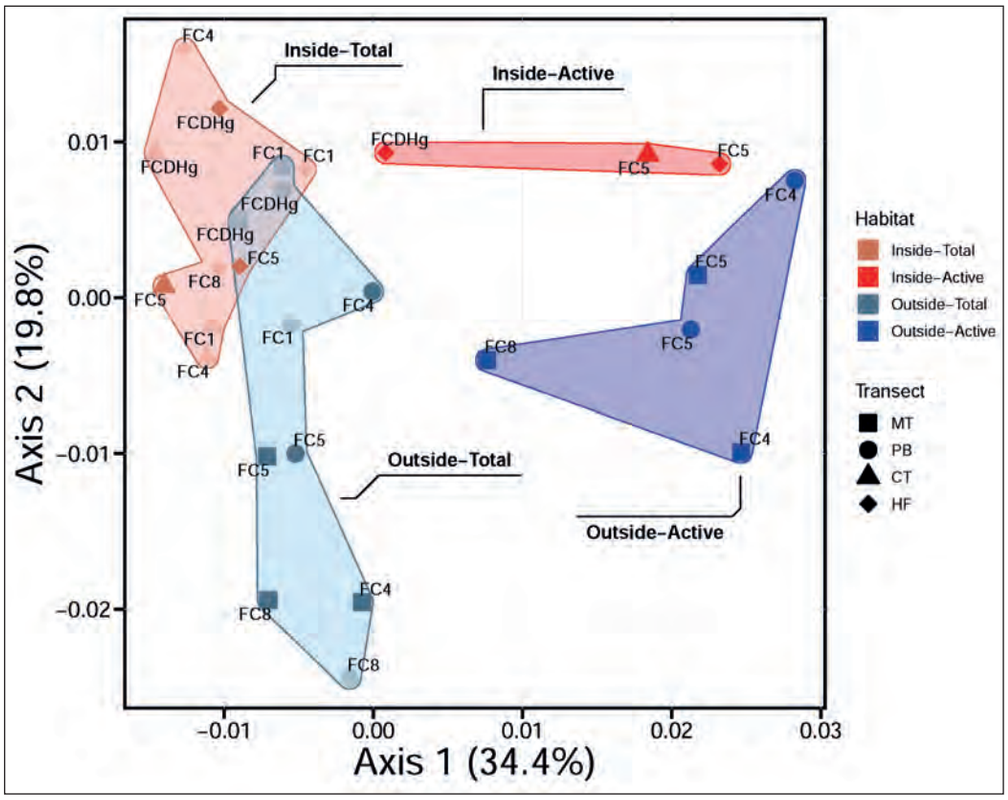

Figure 8.4.3: PCoA ordination (weighted unifrac distances at OTU resolution, 3% dissimilarity level) of total and active bacterial communities in the soils of the fairy circles. Total bacterial community structures were determined using DNA extracts and active community structures using RNA extracts. Inside samples are in reddish, outside samples are in bluish colours. Shadings of active communities are in more intense colour whereas shadings of total communities are in lighter colour. Points with lighter colours represent samples from which only DNA could be extracted.

temperate grassland soils yielded DNA and RNA extracts with significantly higher concentrations (23.7 µg DNA and 9.6 µg RNA per gram of soil; Wüst et al. 2016). Therefore, the low yields of RNA from eight and the failure to extract RNA from 11 fairy circle soils suggest that the activity of microorganisms in the soils of fairy circle is generally low and that the majority of extracted DNA must represent dead or dormant cells. It was possible to obtain amplicons of bacterial 16S rRNA gene transcripts for all samples containing RNA. In contrast, it was not possible to amplify any fungal ITS2 sequences from the eight successful RNA extractions, suggesting that the activity level of fungi in all fairy circle soils investigated in the present study was extremely low.

A multivariate ordination plot of differences in the composition of active and total bacterial communities in the different fairy circle habitats revealed a pronounced difference between the composition of active and total communities which were actually more pronounced than the differences between the communities in the different fairy circle habitats (Fig. 8.4.3). This was supported statistically by a PERMANOVA analysis on the eight samples for which both DNA and RNA were successfully extracted. Although the difference at habitat level (inside versus outside) is already statistically significant (mean PERMANOVA p-value = 0.0115, $R^2 = 0.205$), a larger fraction of the observed variance is explained at the level of total versus active communities ($R^2 = 0.344$) with an even smaller mean PERMANOVA p-value ($p = 0.00117$). Overall, these results indicate that the habitats of fairy circles represent harsh ecological conditions with a substantial effect on the activity status of both bacteria and even more so in fungi.

Bacterial and fungal species diversity

At the level of community composition differences (beta-diversity) a direct comparison of bacterial and fungal community structures was not possible as different target genes (16S rRNA gene sequences and ITS2 sequences, respectively) were used for the amplicon based high-throughput sequencing. However, some measures of alpha-diversity open the possibility to directly compare bacterial and fungal community properties and structures. Alpha-diversity reflects two aspects of the community, richness (the number of species) and evenness (a measure of

the similarity of the relative share of each species in the community) (Tuomisto 2012). Species richness in environmental sequence libraries can be simply quantified as counts of OTUs. Many indices of evenness have been proposed, but there is no consensus which one is the best (Smith & Wilson 1996; Tuomisto 2012). We therefore chose to analyse species-abundance-distributions (SADs) as a proxy for evenness (Su 2018), which describe the distribution of abundances for each different species encountered within a community (McGill et al. 2007). SAD is independent of richness values and has contributed much to the development of (macro-) ecological and biogeographic theories also for microbes (Shoemaker et al. 2017). SADs approximated with gamma-distribution models can numerically be characterized by a single free parameter termed alpha-gambin value (Matthews et al. 2014; Ugland et al. 2007).

The richness of total bacterial communities in the tapetum was slightly (by a factor of 1.13), but statistically significantly ($p < 0.001$), larger than the values in soils from inside or outside of the fairy circles (Fig. 8.4.4A). The within-habitat variability of bacterial richness values in soil and tapetum samples was rather low. In contrast, the range of bacterial richness values in the termite gut samples was large and the average value was considerably lower than in soil or tapetum (by a factor of 0.67, $p < 0.001$). The richness of the eight active bacterial soil communities was statistically significantly lower (on average 0.95-fold; t-test, $p = 0.031$) than the richness of their corresponding total communities, which further supports our notion that soils of fairy circles represent a highly selective environment in comparison to temperate grasslands which often have a higher richness in the active fraction (unpublished results). The richness of the active communities in outside soils was only marginally larger than that from the soils inside fairy circles (1.05-fold; t-test, $p = 0.22$).

In contrast to bacteria, fungal species richness characteristics differed from bacterial richness in the two aspects. First, there was no notable difference in richness values between soil and tapetum samples. Second, the range of within-habitat fungal species richness values was much larger than that of bacteria. However, fungal richness tended to be smaller on average (approx. 0.72-fold) than richness values of bacterial communities.

Compared to richness, the analysis of SADs revealed three important differences among the microbial communities (Fig. 8.4.4B). Firstly, for total bacterial communities, the largest alpha-gambin values were observed for the soil samples which indicates a more even community composed of several dominant species (see also panels 1 and 2 in Fig. 8.4.4C). The tapetum samples showed lower alpha-gambin values than the soil samples (approx. 0.61-fold, $p < 0.001$), suggesting a higher dominance of only few taxa (see panels 3 and 4, Fig. 8.4.4C). The bacterial communities in the termite guts showed the lowest alpha-gambin value which implies that only very few species constitute the vast majority of the community (up to 80%; see panels 5 and 6, Fig. 8.4.4C). Secondly, fungal communities in soils and tapetum were characterized by a very tight range of substantially low alpha-gambin values (Fig. 8.4.4B), irrespective of their observed wide range of richness values (Fig. 8.4.4A). The average alpha-gambin values of fungi in soils inside or outside the fairy circles and of tapetum samples were low (comparable to bacteria in the termites' gut) reaching only 1.04, 0.93 and 0.81, respectively, which indicates a strong dominance of only few fungal taxa in all these communities. Thirdly, the SADs of active bacteria showed mostly (seven out of eight samples; binom test, $p = 0.07$) a lower alpha-gambin value (in average 0.75-fold; t-test p-value = 0.024), thus reflecting an increased dominance (activity) of only few species. The alpha-gambin of the active community from the outside soils is approximately 1.2-fold larger than that from the inside soils, albeit statistically not significant (t-test, $p = 0.35$).

Abundance and habitat prevalence of specific bacterial and fungal taxa

As both, bacterial and fungal total community composition and species diversity level (richness and SADs) differed across the different fairy circle habitats, and for bacteria also between total and active communities, we sought to identify those microbial taxa which are abundant, differ in their abundance across habitats and hence maybe most relevant for the biogeochemical processes in fairy circles. For this purpose, bacterial sequence variants were classified at the genus level since the sequence information contained in 16S rRNA short reads typically is not sufficient for species delineation. For fungi, a total of 122 OTUs covered 95% of the total number of reads from the tapetum

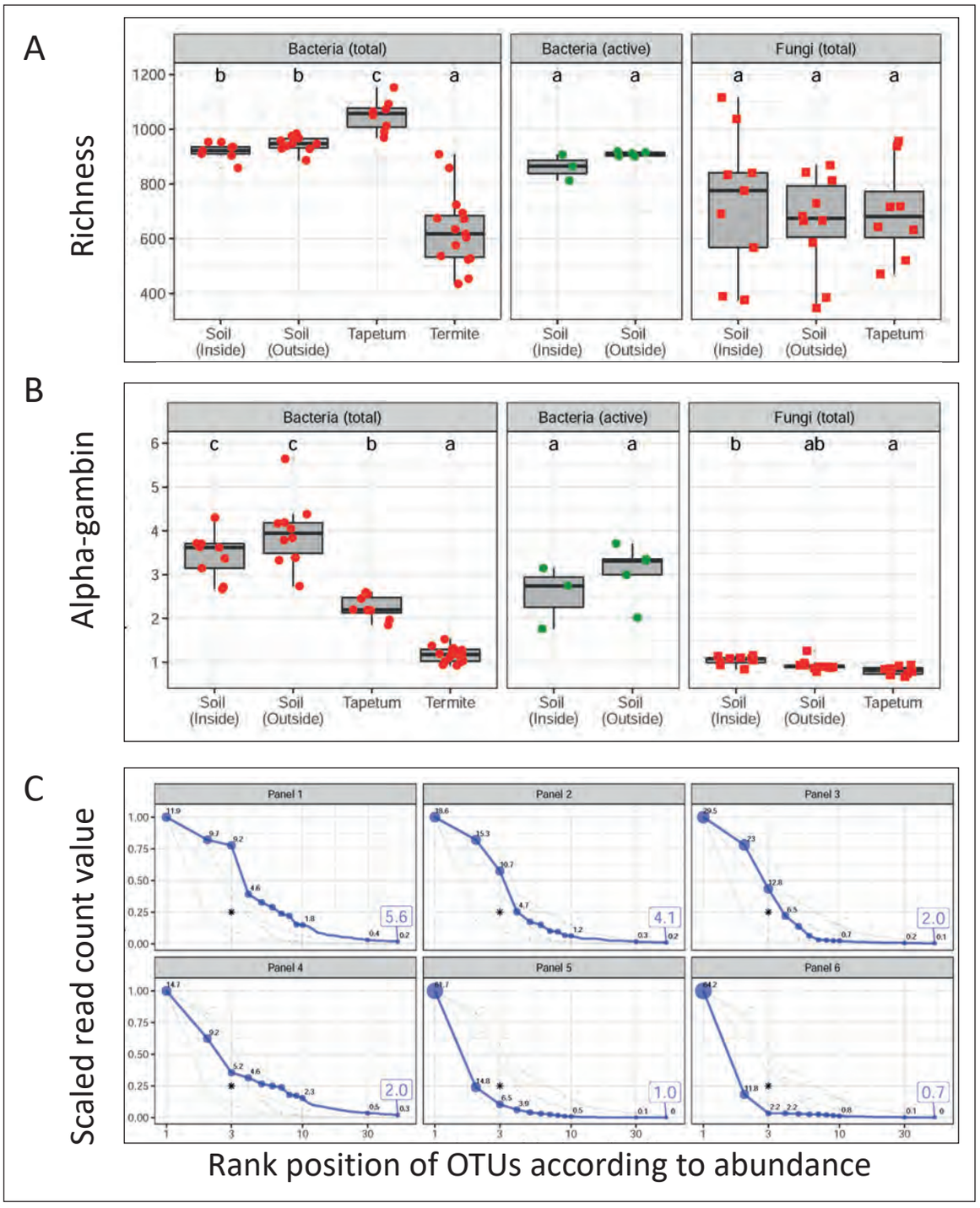

Figure 8.4.4: Richness and species-abundance distributions (SADs) of bacterial and fungal communities.
A: Richness of bacteria and fungi. Each dot represents a sample using the community structure at OTU resolution (3% dissimilarity level). Small letters indicate statistical difference in the mean value significant at p = 0.05.
B: Bacterial and fungal SAD alpha-gambin values. Small letters indicate statistical difference in the mean value significant at *p* = 0.05.
C: Exemplary SAD curves of six individual samples representing the full range from small (0.7, 1.0), intermediate (2.0) to large (4.1, 5.6) alpha-gambin values. Only the 50 most abundant species are shown. All panels show the six SADs curves in grey colour as background curves for direct comparability, whereas one curve and its corresponding alpha-gambin value is highlighted in blue in each of the panels. Read count values of all SAD curves were scaled by setting the read count value of the most abundant OTU to 1. Small black values close to filled circles show the relative abundance (%) of the respective OTU, in addition, the size of the filled taxon circles corresponds to their relative abundance. The value in the coloured label shows the alpha-gambin value. The black star in each panel is at the same x-y position and provides a visual orientation for the difference in curve shape pattern. The larger the alpha-gambin value, the more homogeneous is the abundance distribution of the most abundant taxa. Samples with lower alpha-gambin values are characterized by a higher dominance of the most abundant taxon.

samples. These OTUs were identified to the species level using NCBI GenBank and MycoBank databases; taxonomic assignments follow NCBI Taxonomy. Thirteen of these OTUs were identified as protozoa or represented nonsense sequences. The remaining 109 fungal OTUs made up a total of 92% of total sequence reads.

We observed a strong difference between bacteria (Fig. 8.4.5A) and fungi (Fig. 8.4.5B) in their prevalence pattern across different habitat types. Bacterial genera showed low specificity across all habitat types. Only few of the taxa were detected exclusively in tapetum and termite guts, and in some cases represented a considerable proportion in the termite guts (Fig. 8.4.5A). In contrast, fungi seemed to have a much larger habitat specificity as several OTUs were only detected in specific habitat types (Fig. 8.4.5B). In the case of fungi, and in strong contrast to bacterial taxa, the habitats appear to select much more strongly for specific fungal taxa, both across major habitats (soils versus tapetum), but also at the level of different soils (inside versus outside, Fig. 8.4.5B). This observation is not the result of insufficient sequencing depth since the coverage of OTUs was observed to be high in the alpha-rarefaction analysis (see above). However, because the amplification of active fungal communities failed, the amplification products of total fungal DNA may originate from dead and dormant cells (and spores). Therefore, the viable and potentially active community was further analysed by means of cultivation (see below).

With respect to bacteria, we observed a strong dominance of the single genus *Bacillus* which comprised up to 90% of both the total and active bacterial community. This observation appears to contrast the large alpha-gambin values of the soil samples (Fig. 8.4.4B), but can be explained by the fact that the genus was actually represented in samples by several dominant taxa. Overall, 123 different OTUs of *Bacillus* could be detected, whereas other bacterial genera in the soil samples were represented by much less OTUs (e.g., *Rubrobacter* by 20, *Geodermatophilus* by 10 and *Belneimonas* by only 4 OTUs). The relative abundances of the genus *Bacillus* were even higher in the active community than in the total community, which suggests a strong ecological role of these bacteria in fairy circles rather than a mere persistence as endospores. *Bacillus* was also prominent in the tapetum (dark linings of the tunnel system) but rather rare in the termite guts. In addition to *Bacillus*, *Planomicrobium* constituted another abundant genus in the tapetum. Dominant genera in the termite gut bacterial communities were *Pseudomonas*, *Dysgonomonas* and *Treponema*.

According to the ITS2 amplicon high-throughput sequencing results, the soils of fairy circles contained high number of reads of the fungal genera *Westerdykella*, *Pithomyces*, *Canariomyces*, and *Stachybotrys* (Fig. 8.4.5B). The most species-rich genera were *Curvularia* (N = 3), *Preussia* (3) and *Westerdykella* (3). Among the five most frequently detected species, *Westerdykella centenaria* was a very common species in both, tapetum and soils. Nevertheless, species composition in soils strongly differed from that in tapetum (Fig. 8.4.5B). A large number of OTUs was exclusively present either in the tapetum or soils.

In addition to *Westerdykella centenaria,* which was the most abundant species in tapetum, high abundances of the reads of *Aspergillus terreus*, *Aspergillus flavus*, and *Lichtheimia hyalospora* distinguished tapetum fungal communities from those in soils (Fig. 8.4.5B). Outside soils yielded nearly equal proportions of reads of *Pithomyces cynodontis* and *Westerdykella* sp. (GenBank MG250472). Two other species, *Westerdykella centenaria* and *Stachybotrys microspora* showed nearly equal abundances. Soils inside fairy circles were dominated by a potential new species of the genus *Westerdykella*, while *Pithomyces cynodontis* and another *Westerdykella* sp. (close to *W. ornata*) were detected in equally high abundances.

Sequences of the ten most prominent fungi were largely represented by thermophilic (e.g., *Canariomyces subthermophilus*, *Lichtheimia hyalospora*) and dark-coloured (e.g., *Curvularia*, *Pithomyces*, *Westerdykella*) fungi, some with a pronounced capability to degrade plant material (Berka et al. 2011; Glass et al. 2013; Kubicek et al. 2014; Berlemont 2017). The relative abundance of *Curvularia* species was higher in soils than in tapetum (Fig. 8.4.5B). The presence of *Curvularia* in the termite guts, independently if they were collected inside or outside the fairy circles, was supported by PCR using genus-specific pair primers.

Our results on the observed difference in community composition of bacteria with respect to

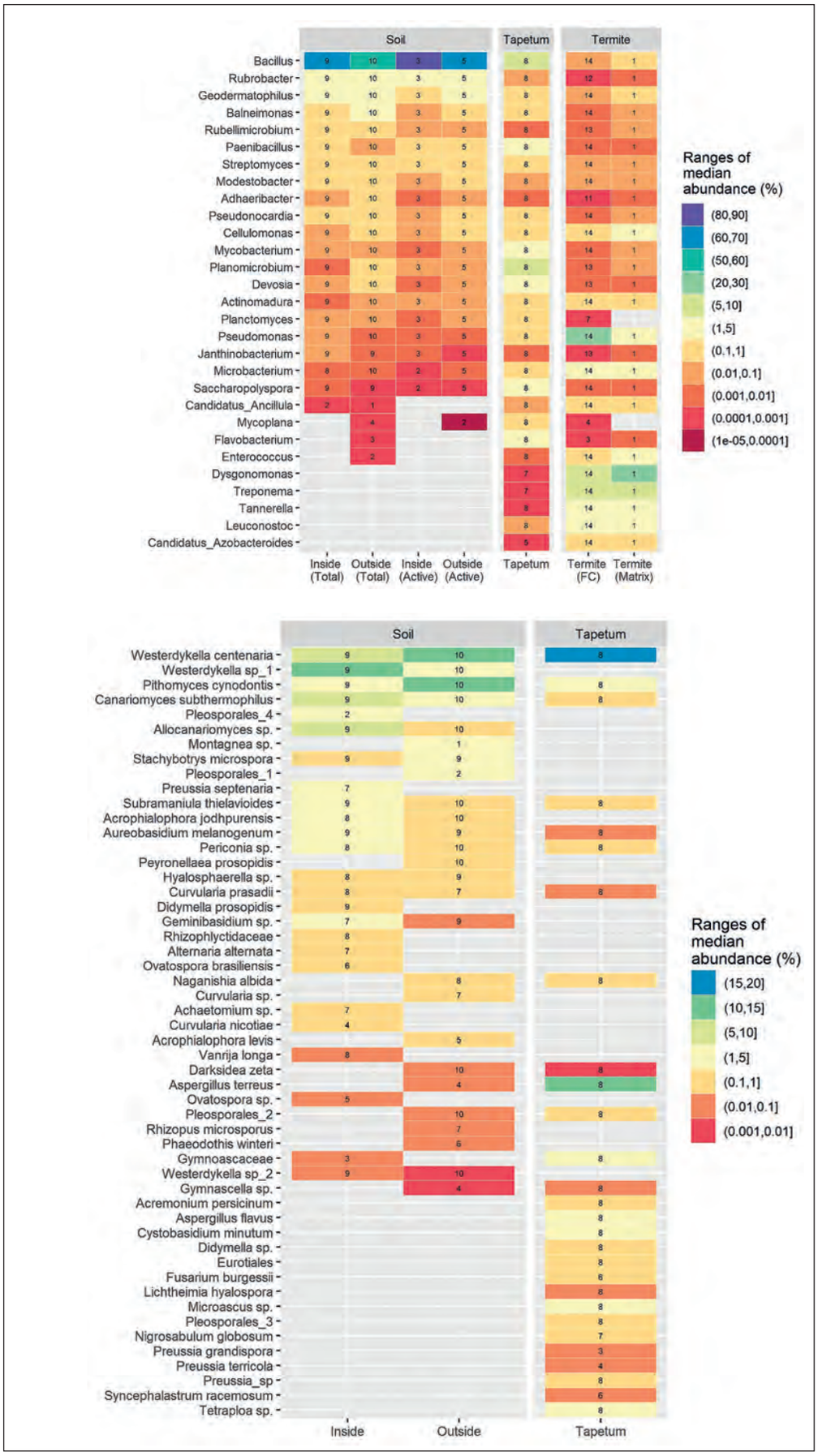

Figure 8.4.5 A and B: Heatmaps of taxon abundances for bacterial genera (A) and fungal species (B). Only the most dominant taxa are shown. The colours reflect median relative abundances across all samples (count values are given as small black values) in which the respective taxa were detected. The median was chosen since the distribution of relative abundance values per taxon across the samples of a habitat type was typically non-normal. The abundance values were binned to ranges, where the lower indicated value is not included in the bin but the upper value is included.

the inside versus the outside of soils samples of fairy circles are in line with few previous studies (Ramond et al. 2014; Van der Walt et al. 2016), but differ with respect to the composition of fungal communities. Our study also provides insights at the level of active bacterial communities and provides for the first time information on microorganisms inhabiting the tapetum of termite burrows as another highly relevant habitat in the fairy circle ecosystem.

All previous studies solely relied on culture-independent molecular approaches but did not assess viability, physiological activity and ecological functions of these microorganisms using isolates (Overmann et al. 2017). The dynamic of the fairy circle ecosystem is believed to be strongly modulated by water availability and termite activity (Jürgens 2013; Jürgens et al. 2015), as also presented in details in Chapter 4 of this book. In order to better understand the involvement of microorganisms in the fairy circle ecosystem, we particularly investigated microbial population of termite nests (Jürgens 2013; Jürgens et al. 2015) in the tapetum material of the tunnel burrows (dark linings for both bacteria and fungi, plant residues only for fungi) of the termite *Psammotermes allocerus*. The fact that many fungi detected by sequencing (ITS2-HTS) are associated with plants suggests that they likely originated from grasses growing in the perennial belt of fairy circles. Because this grass cover is not constant and only reappears after a period of rains, fungi need an alternative refugium (or host) and vector to recolonize grasses in the perennial belt. Thus, we hypothesized that termite nests, which are able to retain water during extended periods of drought lasting over several years (Jürgens 2013), would efficiently support microbial activity in the (poly) extremophile habitat of fairy circles.

Bacterial and fungal isolates retrieved from the tapetum

Overall, 89 bacterial strains were obtained by cultivation, representing a remarkable diversity covering 47 species from 32 genera, 21 families, 11 orders, six classes and four phyla. These strains were taxonomically identified using complete 16S rRNA gene sequences and their nucleotide similarity values of the isolates to those of the next closest validly named bacterial species in the data bases ranged from 93.4% to 100%. Given the lower threshold value of 98.6% for bacterial species discrimination (Meier-Kolthoff et al. 2013), half of the isolated strains represent new species and some even new genera. When comparing the 32 genera obtained as isolates with the bacterial diversity obtained at the molecular level (106 genera, Fig. 8.4.5A), 17 of the cultured genera (Box 8.4.1) could not be detected within the molecular data set obtained from tapetum samples. In addition, only six of the 15 genera which were detected both, in cultured and molecular datasets (Box 8.4.1), also represented the most abundant genera in the molecular data set (*Flavobacterium*, *Microbacterium*, *Devosia*, *Mycobacterium*, *Bacillus*, and *Streptomyces*). Notably, several of the tapetum genera only observed by culturing approaches can be associated with important ecological roles related to plant material: *Rhizobium, Microvirga* and *Ensifer* are nitrogen-fixing bacteria living in association with plant roots and thereby may provide plants with nitrogen. The genus *Cellulosimicrobium* is involved in degradation of plant biomass (Vu et al. 2021), which is probably brought into the tapetum in ample amounts by the termites. Some strains of *Mariniluteicoccus* are endophytic and have been isolated from root material (Liu et al. 2016). Similarly, several species of *Okibacterium* have been isolated from roots and seeds from several plant species (Evtushenko et al. 2002; Wang et al. 2015). Strains of other genera

Bacterial genera cultivated from tapetum:

Bacterial genera jointly detected in cultured and molecular approaches: *Arthrobacter, Bacillus, Devosia, Flavobacterium, Georgenia, Leucobacter, Mesorhizobium, Microbacterium, Mycobacterium, Nocardioides, Parapedobacter, Pedobacter, Rhodococcus, Sphingomonas, Streptomyces*

Bacterial genera only detected in cultured approaches: *Aeromicrobium, Agrococcus, Arsenicitalea, Brevundimonas, Cellulosimicrobium, Ensifer, Isoptericola, Mariniluteicoccus, Marmoricola, Massilia, Methylobrevis, Microvirga, Okibacterium, Psychroglaciecola, Rhizobium, Sphingoaurantiacus, Sphingosinicella*

Box 8.4.1

(*Psychroglaciecola*, *Sphingoaurantiacus*) have been isolated from other harsh environments like arctic glacial foreland soil or arctic tundra soil (Kim et al. 2016; Qu et al. 2014). Thus, the identification of these culturable and consequently viable bacteria suggest a role of plant material in the tapetum of the termite *Psammotermes allocerus* and may represent the causal link between termites and plant degradation with implications for the ecology of fairy circles.

A total of 80 fungal species were isolated from soils inside the fairy circles, the dark lining of the tapetum, plant material stored in the subterranean tunnel system, and from grass samples of the perennial belt. These strains were taxonomically identified using complete ITS and partial LSU rRNA gene sequences, and sequences of protein-coding genes. In line with the failure to amplify and sequence active fungi from the loose sandy soils, these samples yielded only a few isolates, of which the two basidiomycetous yeasts *Cystobasidium minutum* and *Naganishia albida* were most prominent (Table 8.4.2). *Naganishia albida* (syn. *Cryptococcus albidus*) is a prominent soil yeast (Yurkov 2017, 2018). Although its distribution is not restricted to dry habitats (e.g., Yurkov et al. 2015), this species shows a remarkable ability to survive in air-dried autoclaved loamy sand thanks to its thick polysaccharide capsules (Vishniac 1995). *Naganisha albida* was detected in inside and outside soils as well as in tapetum in nearly equal proportion of reads. Yeasts of the genus *Cystobasidium* are halotolerant but psychrophilic (Buzzini et al. 2018). Our isolation of these yeasts from hot and dry sandy soils is intriguing and deserves further studies. Although ITS2 HTS detected diverse fungal communities in fairy circle soils (Fig. 8.4.5B), the results of our cultivation experiments suggest that the vast majority of these fungi are not viable.

Table 8.4.2: Cultivated fungal taxa most frequent in soil within fairy circles, 623 tapetum and plant material from tapetum. Genera and species with 624 probability of isolation above 0.3 are shown

	Probability of isolation	Soil	Tapetum	Plant
Acremonium spp. (4)	0.56		X	
• *A. antarcticum*	0.38		X	X
Alternaria spp. (4)	0.38		X	
Aspergillus spp. (4)	0.63		X	X
• *A. terreus*	0.38		X	X
Aureobasidium melanogenum	0.31		x	
Chaetomium spp. (6)	0.56		X	X
Cladosporium spp. (3)	0.69		X	
Curvularia spp. (10)	2.19			
• *C. carica-papayae*	0.75		X	X
• *C. chlamydos*pora	0.44		X	X
• *C. spicifera*	0.50		X	X
Cystobasidium minutum	0.63	X		
Filobasidium (2)	0.63	X	X	
Filobasidium magnum	0.56	X		
Fusarium spp. (3)	0.75			
• *F. chlamydosporum*	0.44		X	X
Naganishia albida	1.50	X		
Penicillium spp. (4)	0.44		X	
Pithomyces cynodontis	0.94		X	X
Westerdykella spp. (3)	1.81		X	X
• *W. centenaria*	1.56		X	X

During the preparation of samples of tapetum, termite nests were dissected to get access to the dark tapetum lining. The dark lining of tunnels yielded diverse fungal cultures, most of which belonged to the family *Chaetomiaceae*, known soil inhabitants with a pronounced ability to degrade cellulose. Many of these fungi were rarely isolated as indicated by low probability of isolation values (Table 8.4.2). Other fungi occasionally observed in the tapetum probably originated from plants surrounding fairy circles and included plant-related genera *Alternaria*, *Cladosporium*, and *Penicillium* (Table 8.4.2). Tapetum plant material collected from several dead-end compartments of the nest yielded a total of 20 species. The majority of isolates belonged to plant-associated fungi such as members of genera *Curvularia*, *Fusarium*, *Pithomyces* and *Westerdykella*. The genus *Curvularia* was the most species-rich with ten species in total and five species recovered from plant material. Furthermore, *Curvularia* species (*C. chlamidospora*, *C. spicifera*, and *C. carica-papayae*) were the most frequently isolated fungi followed

by *Westerdykella centenaria* and *Pithomyces cynodontis* (Table 8.4.2). Occasionally we also detected thick fungal hyphae growing in tunnels which were identified as *Aspergillus terreus* in an accompanying project (Fig. 8.3.13, this book).

A comparison of cultured and uncultured bacterial and fungal taxa revealed that the cultured bacterial taxa represented only 26% of all detected bacterial taxa. A total of 14% of the bacterial taxa were detected by cultivation only (Fig. 8.4.6 A). This strongly contrasted with the large proportion (63%) of culture-independently determined fungal taxa that was also detected by cultivation (Fig. 8.4.6 B). Nearly half (48%) of all detected fungal taxa were observed only in the cultivated fraction. Our results suggest high habitat specificity of fungi (Figure 8.4.5B). The visual observation of fungi growing in nest tunnels as thick hyphae, together with the high diversity of cultured species in the dark linings of the tapetum (Fig. 8.4.6 C, Table 8.4.2) support our assumption that the environment of termite tunnels, particularly the dark tapetum lining, provides a refugium especially for the fungi of the fairy circles. Although many of these fungi theoretically could survive as spores, conditions in the fairy circle sandy soils likely are too harsh for many of them to survive and establish stable populations.

The link between plants and fungi in the ecological context of fairy circles

Most extremophile fungi can be found on soil and stone crusts in deserts, including both hot and cold Antarctic deserts, and hypersaline environments (Buzzini et al. 2018; Coleine et al. 2022). However, most fungi are not extremely xerotolerant; they produce structures to sustain desiccation but do not actively grow under low water activity regimes (Pitt 1975; Rodríguez-Andrade et al. 2019; Dijksterhuis 2019). The ability to grow at low water activity is limited only to a handful of genera, e.g. *Aspergillus*, *Eurotium*, *Xeromyces*, and *Zygosaccharomyces* (Pitt 1975; Coleine et al. 2022). Our analyses indicated that most of detected fungi (ITS1-HTS) in fairy circle soils were not viable and a few isolated species are known to possess adaptations to drought stress, melanin pigmentation (e.g., *Aureobasidium*), production of exogeneous polysaccharide capsules (e.g., *Naganishia*), and drought-resistant spores (e.g., *Aspergillus*). However, the most frequently detected fungi in soils are not known to be (poly)extremophilic, but are species associated with plant material (Table 8.4.2), either as parasites or degraders (Manamgoda et al. 2011; Berlemont 2017). Their survival in the bare patch soils and the vegetation in the perennial belt disappearing during prolonged periods of drought is highly unlikely according to our cultivation experiments. The diversity of viable, cultivated fungi was substantially higher in tapetum material (both dark linings and plant residues) than in the soils (Fig. 8.4.6 C). Fungal communities in tapetum were characterized by a high taxonomic variability and low evenness (Fig. 8.4.4 B), suggesting that they were rather recruited from the environment and subjected to niche filtering (i.e., selected according to their traits) than result from coevolutionary mutualism relationships, as in the case of termites *Macrotermitinae* (fungus-growing termites) and symbiotic basidiomycetes *Termitomyces* (Aanen et al. 2007; Aanen et al. 2002). Indeed, we did not notice any evidence for a strong association or a cultivation of fungi by *Psammotermes* termites. However, we frequently observed collected and stored grass pieces in the nests' tunnel system. Remarkably, these plant residues were often colonized by plant parasites, as suggested by visible symptoms purplish-brown to black spots with brown centres on plants in the perennial belt of fairy circles (Fig. 8.3.9 and 8.3.10, this book). Based on the successful isolation from these spots, these symptoms were attributed to two prominent necrotrophic pathogens of grasses (*Poaceae*), *Curvularia* and *Pithomyces* (Ahonsi et al. 2010; Eken et al. 2006; Manamgoda et al. 2011; Tóth et al. 2007).

In the past, the closely related genera *Curvularia* and *Bipolaris* (synonyms *Cochliobolus* and *Drechslera*, respectively) have caused devastating fungal infections of important agricultural crops (rice, wheat, maize) (Manamgoda et al. 2011). Several species of *Curvularia* have been isolated and detected in the fairy circle system, which is largely composed of *Stipagrostis* grasses (Van der Walt et al. 2016; this study). In the field, *Curvularia* and *Pithomyces* can result in circular patches resulting from grass dieback (Tomaso-Peterson et al. 2016), the pattern that resembles the shape of fairy circles. Both infections are known to develop in warm climates and are more severe in young and weak plants. Both, broad host range and the reduced plant fitness

in the ecosystem due to the grazing of termites increase chances of fungal infection and die-back in plants reappearing again after rainfall. Jacobson et al. (2015) reported *Psammotermes* termites to graze selectively the outer grey layer of the stems of perennial *Stipagrostis* species infected with fungi, as decomposing plant parts are characterized by a reduced carbon/nitrogen ratio. This observation is in accordance with our results showing the presence of *Curvularia* and *Pithomyces* both via molecular methods (Fig. 8.4.5 B) and, more importantly, as viable cultures from dark linings of tapetum and on plant residues stored in the termite tunnel system (Table 8.4.2). Notably, we detected *Curvularia* fungi also in the termite guts by specific PCR. Our results therefore suggest that termites collect and transport infected leaves to the nest, thereby safeguarding fungal inoculum below ground under favourable conditions (constant water and nutritional regimes) until starting the next infection cycle above ground. Vectored by termites to new plants and inoculated through grazing, necrotrophic plant parasites assist termites keeping fairy circles free of grass. Termites depend on water to survive and profit from plant-free fairy circles, because the fairy circles' bare centres accumulate and preserve belowground water more efficiently, which otherwise will be lost through plant transpiration (e.g., Jürgens 2013).

Conclusions

The determination of active microbial communities through RNA analysis and cultivation approaches revealed that fairly circles represent harsh environments that constrain the diversity of active bacteria and even largely suppress fungal activity. The moister and more nutrient rich tapetum environment constitutes an important refugium for microbes and specifically for fungi. In addition, our findings suggest that *Psammotermes allocerus* acts as vector for plant pathogenic fungi, which are stored in belowground nests as refugium to be transferred later back to surface grasses after rainfalls. Thereby termites may indirectly but substantially contribute to the efficient maintenance of fairy circles.

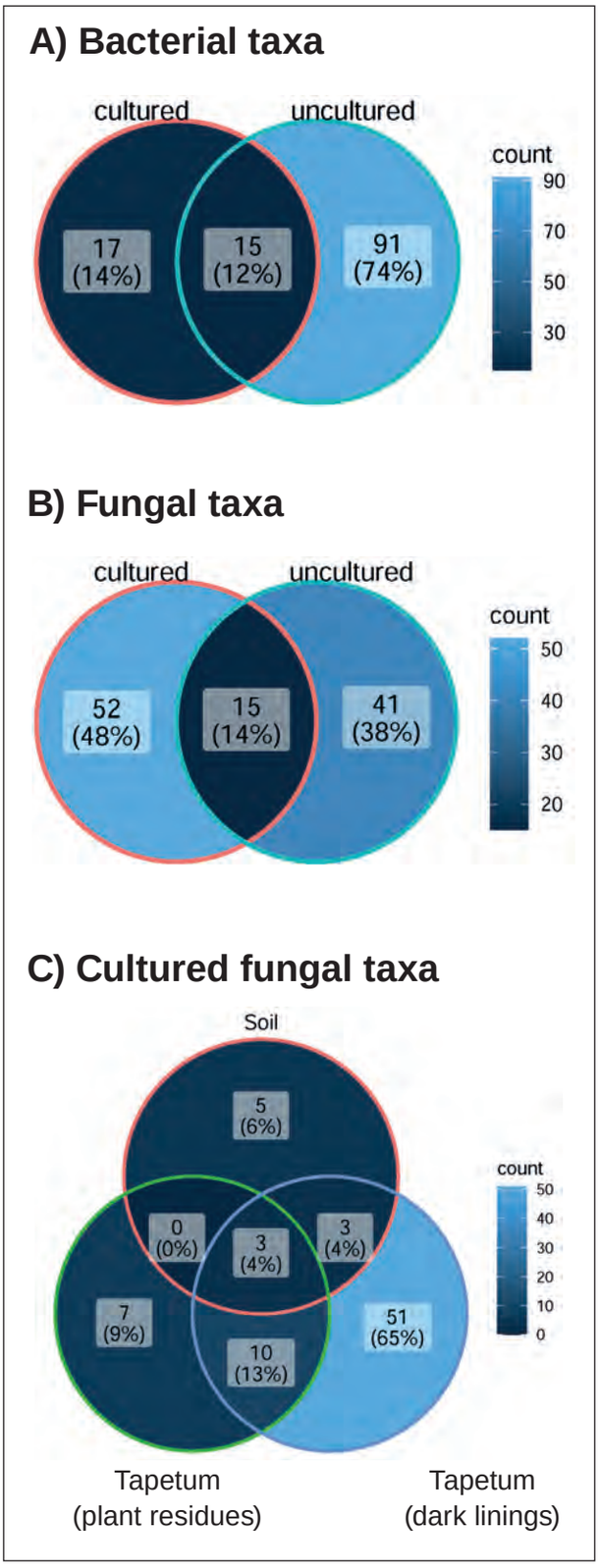

Figure 8.4.6 A, B and C:
Venn diagrams of cultured and uncultured bacterial (**A**, genus level) or fungal (**B**, species level) taxa from the dark linings of tapetum material. (**C**) Venn diagramm of cultured fungal species from different habitats: soil (sand surrounding the nest, CT), tapetum (dark lining), and plant residual material collected from tunnels of the nest.

Acknowledgements

Evelyne Brambilla and Gabrielle Gresenz (DSMZ) are acknowledged for the assistance in the lab. Authors thank Dr. Christiane Baschien (DSMZ) for her valuable advices on culture-independent analyses of fungi. We also thank the Namibian authorities for issuing the necessary permits. The collection of plants, termites and soil samples was done under MET research/collecting permit 1785/2013 (applicant N. Jürgens). The MTA for soil and nests was issued by the NBRI (National Botanical Research Institute) on 22nd April 2014. The export of the termites was under permit Nr. 94229 from 13th October 2013. The export of soil samples was under permit ES 29393 of Ministry of Mines and Energy dating 12th December 2013 and the export of plant material under permit 96776 dating 16th May 2014. The necessary phytosanitary certificates were obtained (Nos. 26110 and 26111, 28th April 2014).

References for Chapter 8.4

Aanen. D. K.. Ros. V. I. D.. de Fine Licht. H. H. *et al.* (2007). Patterns of interaction specificity of fungus-growing termites and *Termitomyces* symbionts in South Africa. *BMC Evolutionary Biology*. **7**. 115–115. doi:10.1186/1471-2148-7-115

Aanen. D. K.. Eggleton. P.. Rouland-Lefèvre. C. *et al.* (2002). The evolution of fungus-growing termites and their mutualistic fungal symbionts. *Proceedings of the National Academy of Sciences*. **99**. 14887–14892. doi:10.1073/pnas.222313099

Ahonsi. M. O.. Agindotan. B. O.. Williams. D. W. *et al.* (2010). First report of *Pithomyces chartarum* causing a leaf blight of *Miscanthus* × *giganteus* in Kentucky. *Plant Disease*. **94**. 480. doi:10.1094/PDIS-94-4-0480C

Armstrong. A.. Valverde. A.. Ramond. J.-B. *et al.* (2016). Temporal dynamics of hot desert microbial communities reveal structural and functional responses to water input. *Scientific Reports*. **6**. 34434. doi:10.1038/srep34434

Berlemont. R. (2017). Distribution and diversity of enzymes for polysaccharide degradation in fungi. *Scientific Reports*. **7**. 222. doi: 10.1038/s41598-017-00258-w

Berka. R.. Grigoriev. I.. Otillar. R. *et al.* (2011). Comparative genomic analysis of the thermophilic biomass-degrading fungi *Myceliophthora thermophila* and *Thielavia terrestris*. *Nature Biotechnology*. **29**. 922–927. doi: 10.1038/nbt.1976

Bokulich. N. A.. Subramanian. S.. Faith. J. J. *et al.* (2013). Quality-filtering vastly improves diversity estimates from Illumina amplicon sequencing. *Nature Methods*. **10**. 57. doi:10.1038/nmeth.2276

Buzzini. P.. Turchetti. B. & Yurkov. A. (2018). Extremophilic yeasts: the toughest yeasts around? *Yeast*. **35**. 487–497. doi:https://doi.org/10.1002/yea.3314

Caporaso. J. G.. Bittinger. K.. Bushman. F. D. *et al.* (2010). PyNAST: a flexible tool for aligning sequences to a template alignment. *Bioinformatics*. **26**. 266-267. doi:10.1093/bioinformatics/btp636

Caporaso. J. G.. Kuczynski. J.. Stombaugh. J. *et al.* (2010). QIIME allows analysis of high-throughput community sequencing data. *Nature Methods*. **7**. 335–336. doi:10.1038/nmeth.f.303

Carini. P.. Marsden. P. J.. Leff. J. W. *et al.* (2016). Relic DNA is abundant in soil and obscures estimates of soil microbial diversity. *Nature Microbiology*. **2**. 16242. doi:10.1038/nmicrobiol.2016.242

Carl. S.. Mohr. S.. Sahm. R. & Baschien. C. (2022). Laboratory conditions can change the complexity and composition of the natural aquatic mycobiome on *Alnus glutinosa* leaf litter. *Fungal Ecology*. **57-58**. 101142. doi:10.1016/j.funeco.2022.101142

Chao. A. & Jost. L. (2012). Coverage-based rarefaction and extrapolation: standardizing samples by completeness rather than size. *Ecology*. **93**. 2533–2547. doi:10.1890/11-1952.1

Coleine. C.. Stajich. J.E. & Selbmann. L. (2022). Fungi are key players in extreme ecosystems. *Trends in Ecology & Evolution*. **37**. 517–528. doi: 10.1016/j.tree.2022.02.002

Costea. P. I.. Zeller. G.. Sunagawa. S. & Bork. P. (2014). A fair comparison. *Nature Methods*. **11**. 359. doi:10.1038/nmeth.2897

Cowan. D. A.. Hopkins. D. W.. Jones. B. E. *et al*. (2020). Microbiomics of Namib Desert habitats. *Extremophiles*. **24**. 17–29. doi:10.1007/s00792-019-01122-7

Delgado-Baquerizo. M.. Eldridge. D. J.. Ochoa. V. *et al*. (2017). Soil microbial communities drive the resistance of ecosystem multifunctionality to global change in drylands across the globe. *Ecology Letters*. **20**. 1295-1305. doi:10.1111/ele.12826

Dijksterhuis J. (2019). Fungal spores: Highly variable and stress-resistant vehicles for distribution and spoilage. *Food Microbiology*. **81**. 2–11. doi: 10.1016/j.fm.2018.11.006

Edgar. R. (2010). Search and clustering orders of magnitude faster than BLAST. *Bioinformatics*. **26**. 2460–2461.

Edgar. R. C.. Haas. B. J.. Clemente. J. C.. Quince. C. & Knight. R. (2011). UCHIME improves sensitivity and speed of chimera detection. *Bioinformatics*. **27**. 2194–2200. doi:10.1093/bioinformatics/btr381

Eken. C.. Jochum. C. C. & Yuen. G. Y. (2006). First report of leaf spot of smooth bromegrass caused by *Pithomyces chartarum* in Nebraska. *Plant Disease*. **90**. 108. doi:10.1094/PD-90-0108C

Evtushenko. L. I.. Dorofeeva. L. V.. Krausova. V. I. *et al*. (2002). *Okibacterium fritillariae* gen. nov.. sp. nov.. a novel genus of the family Microbacteriaceae. *International Journal of Systematic and Evolutionary Microbiology*. **52**. 987–993. doi:10.1099/00207713-52-3-987

Getzin. S.. Yizhaq. H.. Bell. B. *et al*. (2016). Discovery of fairy circles in Australia supports self-organization theory. *Proceedings of the National Academy of Sciences*. **113**. 3551–3556 doi:10.1073/pnas.1522130113

Gich. F.. Janys. M. A.. Konig. M. & Overmann. J. (2012). Enrichment of previously uncultured bacteria from natural complex communities by adhesion to solid surfaces. *Environmental Microbiology*. **14**. 2984–2997. doi:10.1111/j.1462-2920.2012.02868.x

Glass. N.L.. Schmoll. M.. Cate. J.H.D. & Coradetti. S. (2013). Plant cell wall deconstruction by Ascomycete fungi. *Annual Review of Microbiology*. **67**. 477–498. doi:10.1146/annurev-micro-092611-150044

Gossner. M. M.. Lewinsohn. T. M.. Kahl. T. *et al*. (2016). Land-use intensification causes multitrophic homogenization of grassland communities. *Nature*. **540**. 266–269. doi:10.1038/nature20575

Gweon. H. S.. Oliver. A.. Taylor. J. *et al*. (2015). PIPITS: an automated pipeline for analyses of fungal internal transcribed spacer sequences from the Illumina sequencing platform. *Methods in Ecology and Evolution*. **6**. 973–980. doi:10.1111/2041-210X.12399

Herberich. E.. Sikorski. J. & Hothorn. T. (2010). A robust procedure for comparing multiple means under heteroscedasticity in unbalanced designs. *PLoS One*. **5**. e9788. doi:10.1371/journal.pone.0009788

Hsieh. T. C.. Ma. K. H. & Chao. A. (2016). iNEXT: an R package for rarefaction and extrapolation of species diversity (Hill numbers). *Methods in Ecology and Evolution*. **7**. 1451–1456. doi:10.1111/2041-210X.12613

Huber. K. J.. Geppert. A. M.. Groß. U. *et al*. (2017). *Aridibacter nitratireducens* sp. nov.. a member of the family *Blastocatellaceae*. class *Blastocatellia*. isolated from an African soil. *International Journal of Systematic and Evolutionary Microbiology*. **67**. 4487–4493. doi:10.1099/ijsem.0.002318

Huber. K. J. & Overmann. J. (2018). *Vicinamibacteraceae* fam. nov.. the first described family within the subdivision 6 *Acidobacteria*. *International Journal of Systematic and Evolutionary Microbiology*. **68**. 2331–2334. doi:10.1099/ijsem.0.002841

Huber. K. J.. Vieira. S.. Sikorski. J. *et al*. (2022). Differential response of *Acidobacteria* to water content, soil type, and land use during an extended drought in African savannah soils. *Frontiers in Microbiology*. **13**. 750456. doi:10.3389/fmicb.2022.750456

Johnson. M.. Zaretskaya. I.. Raytselis. Y. *et al*. (2008). NCBI BLAST: a better web interface. *Nucleic Acids Research*. **36 Suppl_2**. W5–W9. doi:10.1093/nar/gkn201

Jürgens. N. (2013). The biological underpinnings of Namib Desert fairy circles. *Science*. **339**. 1618-–1621. doi:10.1126/science.1222999

Jürgens. N.. Vlieghe. K. E. P.. Bohn. C. *et al*. (2015). Weaknesses in the plant competition hypothesis for fairy circle formation and evidence supporting the sand termite hypothesis. *Ecological Entomology*. **40**. 661–668. doi:10.1111/een.12266

Kim. M.. Kang. O.. Zhang. Y. *et al*. (2016). *Sphingoaurantiacus polygranulatus* gen. nov., sp. nov., isolated from high-Arctic tundra soil, and emended descriptions of the genera *Sandarakinorhabdus*, *Polymorphobacter* and *Rhizorhabdus* and the species *Sandarakinorhabdus limnophila*, *Rhizorhabdus argentea* and *Sphingomonas wittichii*. *International Journal of Systematic and Evolutionary Microbiology*. **66**. 91–100. doi:10.1099/ijsem.0.000677

Kubicek. C.P.. Starr. T.L. & Glass N.L. (2014). Plant cell wall-degrading enzymes and their secretion in plant-pathogenic fungi. *Annual Review of Phytopathology*. **52**. 427–451. doi:10.1146/annurev-phyto-102313-045831

Kuzyakov. Y. & Blagodatskaya. E. (2015). Microbial hotspots and hot moments in soil: Concept & review. *Soil Biology and Biochemistry*. **83**. 184–199. doi:10.1016/j.soilbio.2015.01.025

León-Sobrino. C.. Ramond. J.-B.. Maggs-Kölling. G. & Cowan. D. A. (2019). Nutrient acquisition, rather than stress response over diel cycles, drives microbial transcription in a hyper-arid Namib Desert soil. *Frontiers in Microbiology*. **10**. 1054. doi:10.3389/fmicb.2019.01054

Liu. B.-B.. Chen. W.. Chu. X. *et al*. (2016). *Marmoluteicoccus endophyticus* sp. nov.. an endophytic actinobacterium isolated from root of *Ocimum basilicum*. *International Journal of Systematic and Evolutionary Microbiology*. **66**. 1306–1310. doi:10.1099/ijsem.0.000880

Lozupone. C.. Lladser. M. E.. Knights. D.. Stombaugh. J. & Knight. R. (2011). UniFrac: an effective distance metric for microbial community comparison. *ISME Journal*. **5**. 169–172. doi:10.1038/ismej.2010.133

Maestre. F. T.. Delgado-Baquerizo. M.. Jeffries. T. C. *et al*. (2015). Increasing aridity reduces soil microbial diversity and abundance in global drylands. *Proceedings of the National Academy of Sciences*. doi:10.1073/pnas.1516684112

Manamgoda. D. S.. Cai. L.. Bahkali. A. H.. Chukeatirote. E.. & Hyde. K. D. (2011). *Cochliobolus*: an overview and current status of species. *Fungal Diversity*. **51**. 3–42. doi:10.1007/s13225-011-0139-4

Matthews. T. J.. Borregaard. M. K.. Ugland. K. I. *et al*. (2014). The gambin model provides a superior fit to species abundance distributions with a single free parameter: evidence, implementation and interpretation. *Ecography*. **37**. 1002–1011. doi:10.1111/ecog.00861

McGill. B. J.. Etienne. R. S.. Gray. J. S. *et al*. (2007). Species abundance distributions: moving beyond single prediction theories to integration within an ecological framework. *Ecology Letters*. **10**. 995–1015. doi:10.1111/j.1461-0248.2007.01094.x

Meier-Kolthoff. J.. Göker. M.. Spröer. C. & Klenk. H.-P. (2013). When should a DDH experiment be mandatory in microbial taxonomy? *Archives of Microbiology*. **195**. 413–418. doi:10.1007/s00203-013-0888-4

Meyer. J. J. M.. Schutte. C. S.. Galt. N.. Hurter. J. W.. & Meyer. N. L. (2021). The fairy circles (circular barren patches) of the Namib Desert - What do we know about their cause 50 years after their first description? *South African Journal of Botany*. **140**. 226–239. doi:10.1016/j.sajb.2021.04.008

Overmann. J.. Abt. B.. & Sikorski. J. (2017). Present and future of culturing bacteria. *Annual Review of Microbiology*. **71**. 711–730. doi:10.1146/annurev-micro-090816-093449

Pascual. J.. von Hoermann. C.. Rottler-Hoermann. A.-M. *et al*. (2017). Function of bacterial community dynamics in the formation of cadaveric semiochemicals during *in situ* carcass decomposition. *Environmental Microbiology*. **19**. 3310–3322. doi:10.1111/1462-2920.13828

Pascual. J.. Wust. P. K.. Geppert. A. *et al*. (2015a). Novel isolates double the number of chemotrophic species and allow the first description of higher taxa in *Acidobacteria* subdivision 4. *Systematic and Applied Microbiology*. **38**. 534–544. doi:10.1016/j.syapm.2015.08.001

Pascual. J.. Wust. P. K.. Geppert. A. *et al*. (2015b). *Terriglobus albidus* sp. nov.. a member of the family *Acidobacteriaceae* isolated from Namibian semiarid savannah soil. *International Journal of Systematic and Evolutionary Microbiology*. **65**. 3297–3304. doi:10.1099/ijsem.0.000411

Paulson. J. N.. Stine. O. C.. Bravo. H. C. & Pop. M. (2013). Robust methods for differential abundance analysis in marker gene surveys. *Nature Methods*. **10**. 1200–1202. doi:10.1038/nmeth.2658

Pitt. J. I. (1975). Xerophilic fungi and the spoilage of foods of plant origin (R. Duckworth Ed.): Academic Press.

Price. M.. Dehal. P. & Arkin. A. (2010). FastTree 2--approximately maximum-likelihood trees for large alignments. *PLoS One*. **10**. e9490. doi: 10.1371/journal.pone.0009490

Qu. Z.. Jiang. F.. Chang. X. *et al*. (2014). *Psychroglaciecola arctica* gen. nov.. sp. nov.. isolated from Arctic glacial foreland soil. *International Journal of Systematic and Evolutionary Microbiology*. **64**. 1817–1824. doi:10.1099/ijs.0.060913-0

Quast. C.. Pruesse. E.. Yilmaz. P. *et al*. (2013). The SILVA ribosomal RNA gene database project: improved data processing and web-based tools. *Nucleic Acids Research*. **41(D1)**. D590-D596. doi:10.1093/nar/gks1219

Ramond. J.-B.. Pienaar. A.. Armstrong. A.. Seely. M. & Cowan. D. A. (2014). Niche-partitioning of edaphic microbial communities in the Namib Desert gravel plain fairy circles. *PLoS One*. **9**. e109539. doi:10.1371/journal.pone.0109539

Ravi. S.. Wang. L.. Kaseke. K. F.. Buynevich. I. V. & Marais. E. (2017). Ecohydrological interactions within "fairy circles" in the Namib Desert: Revisiting the self-organization hypothesis. *Journal of Geophysical Research: Biogeosciences*. **122**. 405–414. doi:10.1002/2016JG003604

Rodríguez-Andrade. E.. Stchigel. A.M.. Terrab. A. *et al*. (2019). Diversity of xerotolerant and xerophilic fungi in honey. *IMA Fungus*. **10**. 20. doi:10.1186/s43008-019-0021-7

Safriel. U.. Adeel. Z.. Niemeijer. D. et al. (2005). Dryland systems. Ecosystems and human well-being: Current state and trends. Island Press, Washington, DC.

Sahagian. D. (2017). The magic of fairy circles: Built or created? *Journal of Geophysical Research: Biogeosciences*. **122**. 1294–1295. doi:10.1002/2017JG003855

Shoemaker. W. R.. Locey. K. J. & Lennon. J. T. (2017). A macroecological theory of microbial biodiversity. *Nature Ecology & Evolution*. **1**. 0107. doi:10.1038/s41559-017-0107

Sikorski. J.. Baumgartner. V.. Birkhofer. K. *et al*. (2022). The evolution of ecological diversity in *Acidobacteria*. *Frontiers in Microbiology*. **13**. 715637. doi:10.3389/fmicb.2022.715637

Smith. B. & Wilson. J. B. (1996). A consumer's guide to evenness indices. *Oikos*. **76**. 70–82. doi:10.2307/3545749

Steven. B.. Phillips. M. L.. Belnap. J. *et al*. (2021). Resistance, resilience, and recovery of dryland soil bacterial communities across multiple disturbances. *Frontiers in Microbiology*. **12**. 648455. doi:10.3389/fmicb.2021.648455

Su. Q. (2018). A relationship between species richness and evenness that depends on specific relative abundance distribution. *PeerJ*. **6**. e4951. doi:10.7717/peerj.4951

Tedersoo. L.. Anslan. S.. Bahram. M. *et al*. (2015). Shotgun metagenomes and multiple primer pair-barcode combinations of amplicons reveal biases in metabarcoding analyses of fungi. *Mycokeys*. **10**. 1–43.

Tomaso-Peterson. M.. Jo. Y.-K.. Vines. P. L. & Hoffmann. F. G. (2016). *Curvularia malina* sp. nov. incites a new disease of warm-season turfgrasses in the southeastern United States. *Mycologia*. **108**. 915–924. doi:10.3852/15-238

Tóth. B.. Csősz. M.. Dijksterhuis. J.. Frisvad. J. C. & Varga. J. (2007). *Pithomyces chartarum* as a pathogen of wheat. *Journal of Plant Pathology*. **89**. 405–408.

Tuomisto. H. (2012). An updated consumer's guide to evenness and related indices. *Oikos*. **121**. 1203–1218. doi:10.1111/j.1600-0706.2011.19897.x

Ugland. K. I.. John. P.. Lambshead. P. J. *et al*. (2007). Modelling dimensionality in species abundance distributions: Description and evaluation of the Gambin model. *Evolutionary Ecology Research*. **9**. 313–324.

van der Walt. A. J.. Johnson Riegardt. M.. Cowan Don. A. *et al*. (2016). Unique microbial phylotypes in Namib Desert dune and gravel plain fairy circle soils. *Applied and Environmental Microbiology*. **82**. 4592–4601. doi:10.1128/AEM.00844-16

Vishniac. H. S. (1995). Simulated *in situ* competitive ability and survival of a representative soil yeast *Cryptococcus albidus*. *Microbial Ecology*. **30**. 309–320. doi:10.1007/BF00171937

Vu. N. T.. Quach. T. N.. Dao. X. T. *et al*. (2021). A genomic perspective on the potential of termite-associated *Cellulosimicrobium cellulans* MP1 as producer of plant biomass-acting enzymes and exopolysaccharides. *PeerJ*. **9**. e11839. doi:10.7717/peerj.11839

Wang. H.-F.. Zhang. Y.-G.. Li. L. *et al*. (2015). *Okibacterium endophyticum* sp. nov.. a novel endophytic actinobacterium isolated from roots of *Salsola affinis* C. A. Mey. *Antonie van Leeuwenhoek*. **107**. 835–843. doi:10.1007/s10482-014-0376-0

Wüst. P. K.. Nacke. H.. Kaiser. K. *et al*. (2016). Estimates of the bacterial ribosome content and diversity in soils are significantly affected by different nucleic acid extraction methods. *Applied and Environmental Microbiology*. **82**. 2595–2607. doi:10.1128/aem.00019-16

Ye. J.. Coulouris. G.. Zaretskaya. I. *et al*. (2012). Primer-BLAST: A tool to design target-specific primers for polymerase chain reaction. *BMC Bioinformatics*. **13**. 134. doi:10.1186/1471-2105-13-134

Yoon. S. H.. Ha. S. M.. Kwon. S. *et al*. (2017). Introducing EzBioCloud: a taxonomically united database of 16S rRNA gene sequences and whole-genome assemblies. *International Journal of Systematic and Evolutionary Microbiology*. **67**. 1613–1617. doi:10.1099/ijsem.0.001755

Yurkov. A. (2017). Yeasts in Forest Soils. *Yeasts in Natural Ecosystems: Diversity* (ed. by P. Buzzini. M.-A. Lachance and A. Yurkov). pp. 87-116. Cham: Springer International Publishing.

Yurkov. A.. Inácio. J.. Chernov. I. Y. & Fonseca. Á. (2015). Yeast biogeography and the effects of species recognition approaches: The case study of widespread basidiomycetous species from birch forests in Russia. *Current Microbiology*. **70**. 587–601. doi:10.1007/s00284-014-0755-9

Yurkov. A. M. (2018). Yeasts of the soil – obscure but precious. *Yeast*. **35**. 369–378. doi:10.1002/yea.3310

Yurkov. A. M.. Kemler. M. & Begerow. D. (2012). Assessment of yeast diversity in soils under different management regimes. *Fungal Ecology*. **5**. 24–35. doi:10.1016/j.funeco.2011.07.004